

Nafion®-sepiolite composite membranes for improved proton exchange membrane fuel cell performance

Christian Beauger, Guillaume Lainé, Alain Burr, Aurélie Taguet, Belkacem Otazaghine, Arnaud Rigacci

▶ **To cite this version:**

Christian Beauger, Guillaume Lainé, Alain Burr, Aurélie Taguet, Belkacem Otazaghine, et al.. Nafion®-sepiolite composite membranes for improved proton exchange membrane fuel cell performance. Journal of Membrane Science, 2013, 130, pp.167-179. 10.1016/j.memsci.2012.11.037 . hal-00777471

HAL Id: hal-00777471

https://minesparis-psl.hal.science/hal-00777471

Submitted on 17 Jan 2013

HAL is a multi-disciplinary open access archive for the deposit and dissemination of scientific research documents, whether they are published or not. The documents may come from teaching and research institutions in France or abroad, or from public or private research centers.

L'archive ouverte pluridisciplinaire **HAL**, est destinée au dépôt et à la diffusion de documents scientifiques de niveau recherche, publiés ou non, émanant des établissements d'enseignement et de recherche français ou étrangers, des laboratoires publics ou privés.

Nafion®-sepiolite composite membranes for improved Proton Exchange Membrane Fuel Cell performance.

Christian Beauger [a,*], Guillaume Lainé [a], Alain Burr [b], Aurélie Taguet [c], Belkacem Otazaghine [c] and Arnaud Rigacci [a]

(a) MINES ParisTech, CEP/EM&P - Center for Energy and Processes - 1, rue Claude Daunesse - 06904 Sophia Antipolis - France
(b) MINES ParisTech, CEMEF (UMR CNRS 7635) - 1, rue Claude Daunesse - 06904 Sophia Antipolis – France
(c) Centre de Recherche CMGD, Ecole des Mines d'Alès, 6 avenue de Clavières, F-30319 ALES CEDEX

* corresponding author, christian.beauger@mines-paristech.fr, tel : +334 93 95 75 67, fax : +334 93 95 75 35

Abstract
Nafion®-sepiolite composite membranes were prepared, characterized and integrated in Membrane-Electrodes Assembly to be tested in fuel cell operating conditions. The influence of the sepiolite content and its modification on the membrane properties was carefully analyzed. The performances of the different MEAs were compared at different operating temperatures and under various relative humidity.
The sulfonation of pristine sepiolite has improved its ion exchange capacity as well as that of composites membranes. The introduction of sepiolite in Nafion® also allowed simultaneously to increase its water uptake and to improve its mechanical features. Much better performances were obtained at high temperature and low relative humidity with MEAs based upon Nafion®-sepiolite composite membranes compared to pure Nafion® membranes (50 % more output power at 100 °C and 50 %RH).

Keywords: Sepiolite, Nafion, membrane, low humidity, PEMFC

1. Introduction

Due to their wide range of possible applications (transport, mobile or stationary), Proton Exchange Membrane Fuel Cells (PEMFC) are amongst the most studied fuel cells (FC). Nevertheless, despite numerous advanced research studies, they still suffer from limitations. One of them concerns the electrolytic membrane employed so far which impedes the fuel cell to operate at high temperature. Different strategies have been followed to overcome the limitation of Nafion®, the perfluorinated ionomer widely chosen as the standard for PEMFC [1,2,3]. Non-fluorinated polymers such as PEEK [4,5,6], PSU [7,8] or PBI [9,10,11,12] and their sulfonated counterparts have been extensively studied as alternatives. Another strategy consists in incorporating inorganic fillers such as metal oxides [13,14,15,16,17,18,19,20,21], acids [22,23,24,25,26], phosphates or phosphonates [27,28,29] into the Nafion® matrix to make the composite or hybrid membrane more mechanically stable, less permeable to reactant and more hygroscopic. Different clays, montmorillonite [30,31,32] or laponite [33] for instance, have also been evaluated as possible fillers. Palygorskite and sepiolite are fibrous clays known to be very hygroscopic and whose acicular morphology may help to make

composite membranes more mechanically resistant. Palygorskite has already been used as promising filler in Nafion® [34]. In comparison with pristine Nafion® membrane, the composite realized with Nafion® and palygorskite has shown several advantages such as a higher water uptake, both improved mechanical properties and proton conductivities at 0 %RH. However the composite membrane was not tested in a membrane-electrode assembly.

Similarly to palygorskite, the structure of sepiolite is highly porous. This hydrated magnesium silicate ($Si_{12}Mg_8O_{30}(OH)_4(H_2O)_4$, $8H_2O$) is based on SiO_4 tetrahedra layers, with an inversion of the apical ends every six units (Figure 1).

These layers are interconnected by MgO_6 octahedra, thus creating nanochannels of 3.5x10.6 Å² in cross-section [35]. Two types of water molecules are present in the structure: water coordinated to Mg^{2+} ions at the edges of the octahedral layers ($H_2O_{coord.}$) and zeolithic water in the channels ($H_2O_{zeol.}$), hydrogen-bonded to coordinated water molecules.

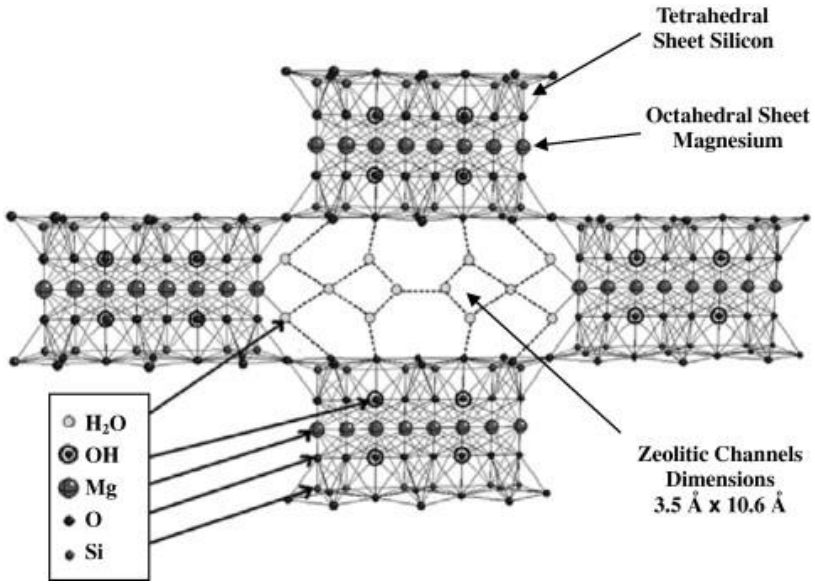


Figure 1: schematic representation of the sepiolite structure after Chivrac et al.. Reprinted from [36] with permission from Elsevier.

Sepiolite, seldomly used as fillers in proton exchange membranes [37,38,39], was chosen to improve the performance of Nafion®. Different composites membranes have been prepared, characterized and used to form Membrane Electrodes Assemblies (MEA). These MEA were then tested in single cell under PEMFC specific operating conditions in order to clearly show the advantage of sepiolite for high temperature and low relative humidity. The cross-influences of the relative humidity of the feeding gases and the operating temperature of the cell were evaluated on the MEA behaviour.

2. Experimental

2.1 Cast Membranes preparation

The membranes were prepared by evaporation of the solvent from a Nafion® dispersion. Starting from a 20 wt% dispersion (ION POWER, DE2021), a 5 wt% dispersion was prepared, using 1-propanol (Fluka 98%), and used to realize both pure and composite membranes. In the case of composites, the sepiolite (Tolsa PangelS9) was added to the dispersion and dispersed with ultrasounds (Bandelin UW2200, 70 W for 1 min, 3 times). The 13x13 cm² mold containing the dispersion was first heated at 80 °C for 2 h and then at 120 °C for 1 h. The obtained membrane was recovered by immersion of the glass support in deionised water. It was finally washed and protonated as follows : 1 h in boiling 0.5 M nitric

acid (HNO_3 Riedel-de Haën 69%), 1 h in boiling 5% hydrogen peroxide (H_2O_2, Fluka 30%) and 1 h in boiling 0.5 M sulphuric acid (H_2SO_4, Aldrich 95-98%). Before being characterized and tested each membrane was stored in deionised water.
Two membranes of each composition were elaborated, one for characterization, the other one for single-cell test.

2.2 Sepiolite sulfonation and characterization

Due to the discontinuity of the layers, numerous OH groups are available for condensation reaction. Tartaglione et al. [40] have reported that the specific number of OH groups equals 2.2 per 100 Å². Based on the specific surface area provided by Tolsa for sepiolite Pangel S9 (S_{BET} = 320 m²/g), the maximum number of OH groups per gram of sepiolite can be estimated to 1.2 mmol/g.

The sulfonation of sepiolite was realized following two protocols.
The first one (#1) was described previously by Fernandez-Carretero et al. [37]. In this protocol, the first step consisted in grafting phenyl-silane groups on sepiolite through condensation reactions between the hydroxyl groups present at the surface of the sepiolite and triethoxyphenylsilane. Hydrochloric acid (3 ml) and isopropanol (17 ml) were added to sepiolite (1 g) under magnetic stirring. Triethoxyphenylsilane (0.6 g) was added after ultrasonic homogenization (Bandelin UW2200, MS73 microtip, 70 W, 90 s). The mixture was heated 15 h at 65 °C, filtered and washed successively with methanol (50 ml), methanol and water (50 ml 50/50) and water (50 ml). The modified sepiolite was finally dried at 90 °C for 2 h and ground in an agate mortar.
The second step consisted in the sulfonation of the phenyl group. The modified sepiolite was treated with fuming sulfuric acid (50 g) under magnetic stirring at 40 °C for 24 h, filtered and washed twice with water at room temperature and then washed three times with water at 50 °C. The so-obtained modified sepiolite (sepiolite#1) was finally dried again at 90 °C for 2 h and grounded in an agate mortar.
The second protocol (#2) is based on a new procedure developed in our laboratory. The first step of this procedure consisted in the functionalization of fillers by an epoxy group. 10 g of sepiolite, 1 g (4.2×10^{-3} mol) of (3-glycidyloxypropyl)trimethoxysilane and 100 ml of an ethanol/water (90/10) solution were introduced in a 250 ml flask fitted with a condenser. The mixture was then stirred and heated at solvent reflux for 15 hours. The mixture was next centrifuged (speed: 400 rpm) to eliminate the liquid phase and washed three times with acetone. The epoxy modified sepiolite was dried under vacuum.
The second step consisted in the introduction of the $-SO_3Na$ group on the epoxy functionalized sepiolite. 10 g of previously epoxy modified sepiolite, 1 g (5.1×10^{-3} mol) of sodium 4-aminobenzenesulfonate and 80 ml of methanol were introduced in a 250 ml flask fitted with a condenser. The mixture was then stirred and heated at methanol reflux for 15 hours. The mixture was next centrifuged (speed: 400 rpm) to eliminate the liquid phase. The treated filler was washed two times with deionised water to remove non reacted sodium 4-aminobenzenesulfonate and two times with acetone. The $-SO_3Na$ functionalized sepiolite was dried under vacuum.
The last step was the modification of the $-SO_3Na$ functionalized sepiolite into a $-SO_3H$ functionalized sepiolite. 5 g of a $-SO_3Na$ functionalized sepiolite and 200 ml of deionised water were introduced in a 500 ml flask. The mixture was stirred and the pH was adjusted to 3 with a 0.01 M H_2SO4 solution. The mixture was centrifuged (speed: 400 rpm) to isolate the treated filler and then washed three times with deionised water and two times with acetone. The $-SO_3H$ functionalized fillers (sepiolite#2) was dried under vacuum.
Both modified sepiolite obtained from protocol #1and #2 are represented on Figure 2.

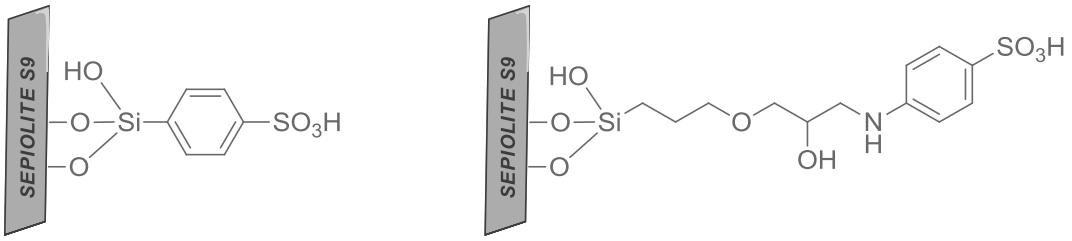


Figure 2: Sulfonated sepiolites obtained by protocol #1 described by Fernandez-Carretero et al. [37] (left) and developed in our laboratory #2 (right).

The functionalization has been checked by thermogravimetric analysis (TGA), infrared spectroscopy, pyrolysis coupled to Gas Chromatography and Mass Spectroscopy (Py-GC/MS) and finally titration. The modification protocol#2 was validated on silica nanoparticles (SIDISTAR® from Elkem).

Thermal characterization was carried out by thermogravimetric analysis (Perkin Elmer Pyris-1 instrument) on 10 mg of samples, under nitrogen. Samples were first heated at 10 °C/min from 25 to 110 °C, followed by an isotherm at 110°C for 10 min, in order to evacuate all adsorbed water molecules. They were then heated again from 110 to 900°C, at 10 °C/min, in order to eliminate grafted groups.

Infrared spectroscopy was performed on a Bruker tensor 27 in ATR mode.

The Py-GC/MS analytical setup consisted of an oven pyrolyzer connected to a GC/MS system. A Pyroprobe 5000 pyrolyser (CDS Analytical) was used to flash pyrolyze the samples in a helium environment. This pyrolyzer is supplied with an electrically heating platinum filament. One coil probe enables the pyrolysis of samples (less than one mg) placed in quartz tube between two pieces of rockwool. The sample was heated at 900 °C for 15 s then the gases were drawn to the gas chromatograph for 5 min. The pyrolysis interface was coupled to a 450-GC gas chromatograph (Varian) by means of a transfer line heated at 270 °C. In this oven the initial temperature of 70 °C was held for 0.2 min, and then raised to 250 °C at 10 °C/min. The column is a Varian Vf-5ms capillary column (30 m × 0.25 mm) and helium (1 ml/min) was used as the carrier gas, a split ratio was set to 1:50. The gases were introduced from the GC transfer line to the ion trap analyzer of the 240-MS mass spectrometer (Varian) through the direct-coupled capillary column. Identification of the products was achieved comparing the observed mass spectra to those of the NIST mass spectral library.

Titration has been carried out following a standard protocol. The fully protonated sepiolite was immersed in 50 ml of 0.001 M NaOH (solution prepared from Acros organics pellets) and 0.1 M NaCl (Sigma Aldrich S3014) in order for the Na^+ ions to replace the H^+ of the sulfonated groups, which thus make the solution pH increased. The remaining HO^- ions were then titrated with 0.001 M HCl (prepared from 1M HCl Fluka 84425), thus allowing to calculate the number of protons exchanged. The IEC is expressed as the number of millimoles of protons exchanged per gram of dry sepiolite (meq/g).

2.3 Membrane Electrodes Assembly

In order to be tested in fuel cell operating conditions, the Nafion®/sepiolite composite membranes were integrated in a Membrane Electrodes Assembly (MEA). To do so, the membrane was hot pressed between two electrodes (Paxitech, 50 cm^2, 0.6 $mgPt/cm^2$) according to the following procedure: 2 metric tons (i.e. 40 kg/cm^2) at 100 °C for 15 min and 10 tons (i.e. 200 kg/cm^2) at 120 °C for 10 min, free cooling at 10 metric tons (press CARVER model 3850).

2.4 Membranes characterizations

2.4.1 Water uptake

The water uptake (W_{ut}) was measured from the difference of the weight of a membrane stored in water at room temperature W_w, and that of the same membrane dried out at 80 °C for 15 h, W_d, according to the following formula, $W_{ut}= (W_w-W_d) /W_d \times 100$.

2.4.2 Swelling

In the presence of water, membranes tend to swell, leading to mechanical constraints in the fuel cell, all the more important as more MEAs are stacked. The swelling (S_i) was measured as the percentage of size increase in the direction i of the membrane (i=1 for side 1, 2 for side 2 and th for the thickness). These percentages were calculated by difference between the size measured after equilibration of the membrane in water at room temperature (RT) on one hand and boiling water (BT) on the other hand. Hence, S_i the swelling percentage in the direction i was calculated as followed: $S_i=100\times[(x_i)_{BT} - (x_i)_{RT}] / (x_i)_{RT}$, where $(x_i)_{BT}$ is the length (in cm) of the membrane in the direction i in boiling water and $(x_i)_{RT}$ is the length (in cm) of the membrane in the direction i in water at room temperature. For the thickness swelling, we have $S_{th} = 100\times (th_{BT}-th_{RT})/th_{RT}$, th being the thickness measured in µm.

2.4.3 Ion Exchange Capacity (IEC)

The IEC was measured by titration according to the procedure described in 2.2. The fully protonated membrane was immersed in 0.1 M NaOH (20 ml solution prepared from Acros organics pellets) The remaining HO^- ions were titrated with 0.01 M HCl (prepared from 1M HCl Fluka 84425).

2.4.4 Microscopies (SEM)

Microscopic observations were realized on FEI XL30 ESEM equipped with a qualitative chemical analysis probe (EDS) to evaluate the sepiolite dispersion within the Nafion® matrix.

2.4.5 Mechanical tests

Mechanical tests were performed in order to control the influence of the fillers on the mechanical resistance of the membrane, which is closely related to its durability in FC operating conditions. Dynamic Mechanical Analysis, performed on a TRITEC 2000 in tensile mode, allowed to determine the Elastic modulus (E). The measurements were realised at 1Hz and at a heating rate of 2 °C/min between 25 °C and 250 °C.

2.5 MEA characterizations

MEAs were tested on our Fuel Cell test bench, controlled by a Biologic potentiostat HCP 803. This Lab equipment allows testing 50 cm² active surface area MEA up to 100 °C, at different stoechiometry and various relative humidity. The polarization curves (U=f(j)) were performed at 75 and 100 °C and between 25 and 100% relative humidity (RH) as described in an earlier publication [41]. These tests also allowed having access to the MEA resistance and the membrane hydrogen crossover.

First of all, the MEA needed to be conditioned to reach their optimum performance. Generally speaking, conditioning tests consist in applying specific operating cycles to the MEA, controlling either the voltage or the intensity. In the context of this study, we chose to apply the following cycle:

- 3 round trips at 5 mV/s, from the Open Circuit Voltage (OCV) down to 0.3 V
- One step at 0.5 V from OCV (5 mV/s), during 1.5 h (no significative evolution of the current afterwards)

3. Results and discussion

3.1 Sepiolite characterization

In order to check to what extent sepiolite has been modified, pristine sepiolite, sepiolite#1 and #2 have been characterized by TGA, IR spectroscopy, Py-GC/MS and titration.

As detailed by several authors [35,42], the heating of pristine sepiolite reveals a multi-step dehydration process, corresponding to the loss of zeolitic water first and then of coordinated water. The zeolitic water is lost in one step, between room temperature and 100 °C, while the coordinated water is lost in two steps, between 100 and 300 °C first and then between 300 and 600 °C. Another step is then observed, from 800°C, corresponding to the dehydroxylation of sepiolite anhydride which loses its structure, resulting in the formation of enstatite and silica.

Thermal characterization of pristine sepiolite and both sulfonated sepiolites (8.25 mg for sepiolite#1 and 11.7 mg for sepiolite#2) was carried out by TGA, following the protocol described in the experimental section. The isotherm step at 110 °C was used to dry samples so as to avoid any disturbance of the results by the weight loss due to the zeolitic water (Figure 3.a). During this step, pristine sepiolite undergoes an 8.4 % weight loss (zeolitic water loss). In the case of organo-modified sepiolites, following protocol #1 and #2, the weight loss is lower compared to pristine sepiolite: 7.2 % and 3.8 %, respectively.

This can be explained by (i) a lower amount of zeolitic water in the organo-modified sepiolite and/or (ii) a higher molecular weight of modified sepiolite due to the presence of organic molecules.

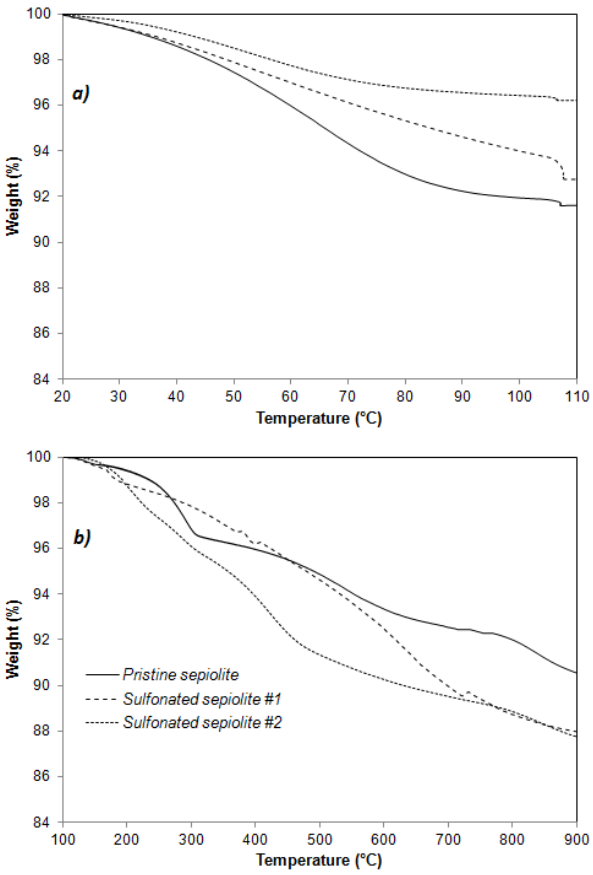


Figure 3: TGA under nitrogen of pristine sepiolite and sulfonated sepiolites (protocols #1 and #2), a) from 25 to 110°C at 10°C/min followed by an isotherm at 110°C for 10 min, b) from 110 to 900°C at 10°C/min.

Considering that all the samples are in the same hydration state after the first step (loss of the zeolitic water), the comparison of their behavior between 110 °C and 900 °C (Figure 3.b) allows checking to what extent the sepiolites have been modified.

The first two steps observed, between 110 °C and 800 °C on Figure 3.b, for pristine sepiolite (straight line) corresponds to a weight loss of 7.5 wt%. They can be attributed to the loss of coordinated water (dehydration). Then, after 800 °C, dehydroxylation occurs.

Between 110 °C and 800 °C, the modified sepiolites #1 and #2 show significantly different behaviors from that of pristine sepiolite but also one from the other. Their behavior is however similar to that of pristine sepiolite above 800 °C, probably corresponding also only to dehydroxylation.

Between 110 and 800 °C the total weight loss of sepiolites #1 and #2 is roughly 11 wt%, i.e. 3.5 wt% more than that of pristine sepiolite. This is a first indication that the sepiolites have been modified. Such a weight loss increase corresponds to 0.3 mg for sepiolite#1 and 0.4 mg for sepiolite#2, ie 0.2 mmol of functional groups per gram of sepiolite#1 and 0.1 mmol of functional groups per gram of sepiolite#2. The calculation was performed assuming that only the silane function of the grafted molecule remains on the mineral filler and that all the organic part was decomposed without char formation.

In order to clarify whether the precursors used are grafted at the surface of sepiolite or trapped in its porosity, both modified sepiolites have been analysed by FTIR spectroscopy and their spectra compared to that of pristine sepiolite (Figure 4).

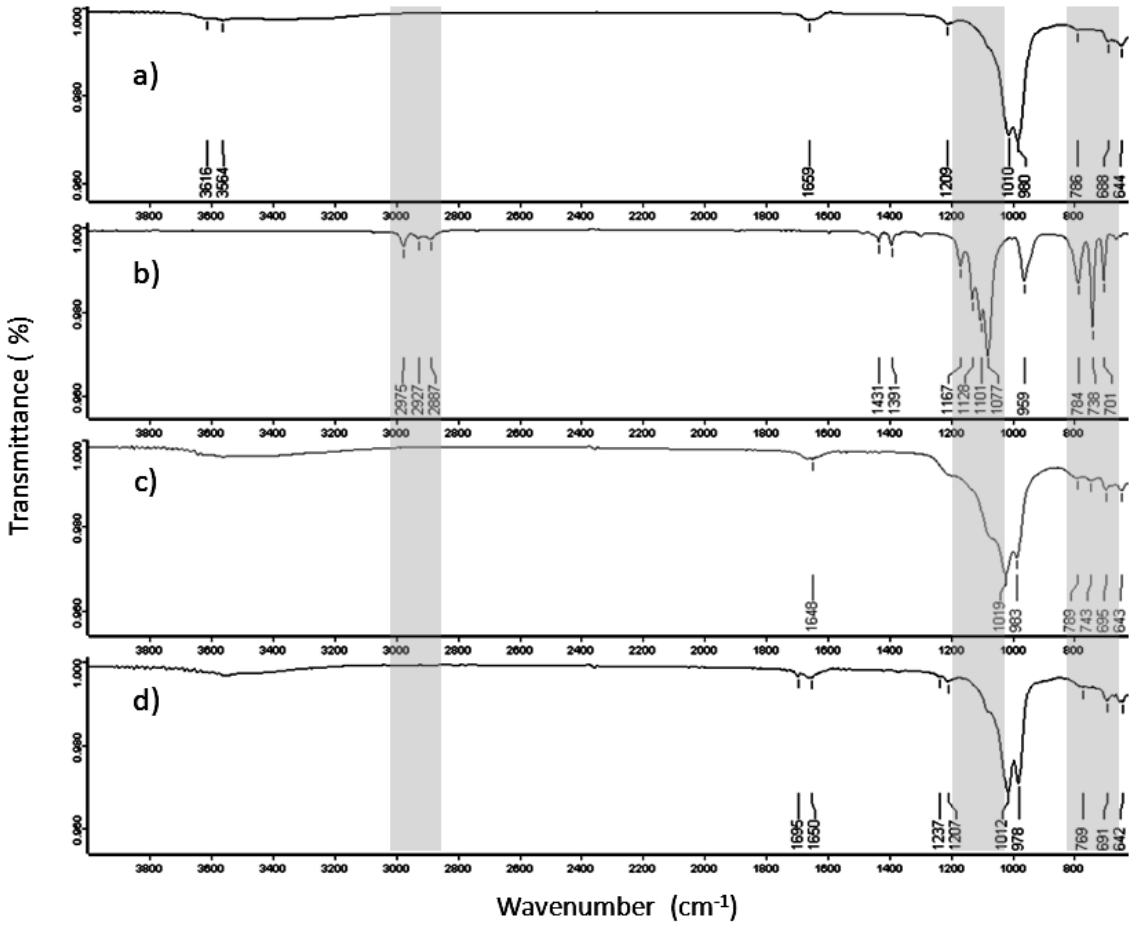


Figure 4: ATR-FTIR spectra of a) pristine sepiolite, b) triethoxyphenylsilane, c) sepiolite#1 and d) sepiolite#2

On the spectrum of pristine sepiolite (Figure 4.a) OH stretching vibrations from Mg_3OH classically appear in the 3600 cm^{-1} region. The bands at 980, 1010 and 1209 cm^{-1} are ascribed to Si-O bonds within silica tetrahedra [43]. Their shift in both modified sepiolites is an indication of an interaction between the grafted group and sepiolite. The band around 1650 cm^{-1} is attributed to water molecules hydrogen bonded to the surface. Finally the bands appearing at 786, 688 and 644 cm^{-1} are also attributed to OH vibrations from Mg_3OH (deformation at 786 cm^{-1} and bending at 688 and 644 cm^{-1}) [44].

Sepiolite#1 shows an additional infrared absorption band around 1080 cm^{-1} (Figure 4.c), which could be attributed to the new Si-O bond coming from the grafted phenyl silane. It may also result from the formation of silica. The bands at 738 cm^{-1} observed for the precursor is also present in sepiolite#1, at 743 cm^{-1} and may be ascribed to the Si-phenyl bond. In the same time, the absorption bands corresponding to the C-H vibrations of the ethoxy groups, at 2887, 2927 and 2975 cm^{-1}, disappeared in the spectrum of sepiolite#1. Since these ethoxy groups from the precursor are expected to be eliminated during the condensation reaction, and considering the weight losses observed in TGA, we concluded that the phenylsilane has been grafted on sepiolite.
Concerning sepiolite#2, the FTIR spectrum shows also an additional absorption band around 1080 cm^{-1}, similar to that observed for sepiolite#1 but weaker. This is probably due to a smaller functionalization, consistent with TGA results. As for sepiolite#1, there is no absorption band in the region of methoxy C-H vibrations, showing that the precursor, here (3-glycidyloxypropyl)trimethoxysilane has reacted with sepiolite OH groups.
In both cases, the absence of C-H vibration bands in the region [2900-3000 cm^{-1}] is a clear indication that the modifications observed cannot come from trapped precursor molecules.

Py-GC/MS analysis has been carried out in order to confirm again the expected surface modifications.

The Py-GC/MS analysis shows for both protocols the release of organic molecules resulting from the decomposition of groups expected to be grafted on sepiolite (Figure 5).

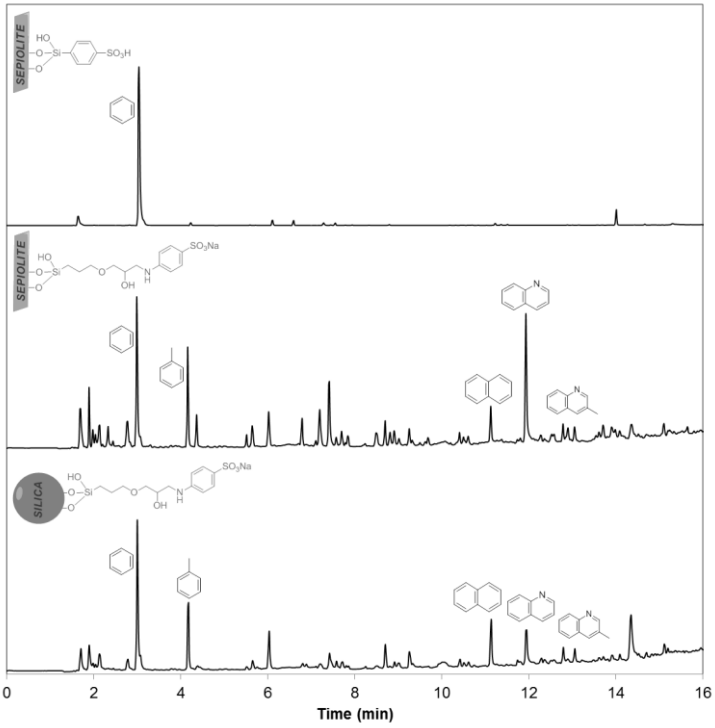


Figure 5: Py-GC/MS chromatograms obtained for sulfonated sepiolites (protocols #1 &2) and silica (protocol #2).

As expected, the pyrolysis at 900°C of the sepiolite sulfonated with the protocol #1 shows mainly a release of benzene which is a clear signature of the group grafted on sepiolite#1.

The chromatogram obtained for the sepiolite #2 shows large differences in comparison to sepiolite #1. The pyrolysis of this modified sepiolite gives a greater variety of molecules. Most of them contain aromatic rings which are formed during the degradation process at high temperature. The presence of nitrogen in some of them is a good indication of a proper functionalization.

Since i) FTIR signal is quite weak for sepiolite#2, probably due to a limited functionalization, and ii) both TGA and Py-GC/MS results could also result from precursor molecules trapped in the sepiolite channels, the procedure of surface modification with protocol#2 has been validated with spherical silica nanoparticles (SIDISTAR® from Elkem).

The chromatogram obtained for silica#2, pyrolised at 900 °C, is very similar to that of sepiolite #2, which proves the formation of the same products during the pyrolysis step of the analysis. Since the precursor could not be trapped in any silica porosity, the detected organic fragments do result from the degradation of groups grafted at the surface of silica. The grafting protocol is thus validated on silica and we can reasonably assume that it is also efficient for sepiolite.

The degree of sulfonation has finally been checked by titration for each modified sepiolite. The results are reported in table 1, along with the data obtained from TGA analysis.

Table 1: TGA and titration results used to calculate the concentration of $–SO_3H$ groups grafted at the surface of sepiolite following protocol#1 and #2.

Sample	**Weight loss due to the drying step (wt%)**	**Weight loss attributed to the grafted part (wt%)**	**-SO_3H concentration (mmol/g)***	
			Calc. from TGA degradation step	Calc. from titration
Pristine sepiolite	8.4	7.5	-	0.03
Sepiolite #1	7.2	11	0.2	0.25
Sepiolite #2	3.8	11	0.1	0.13

** concentration expressed in mmol/g to be compared to the IEC of the membranes*

The concentration of $–SO_3H$ groups obtained for both modified sepiolites are consistent with those obtained with TGA, validating again the two grafting protocols.

The characterisations performed on both modified sepiolites allowed to demonstrate that the grafting protocols were successful. They also revealed that sepiolite#1 is more sulfonated than sepiolite#2 with -SO_3H concentration respectively of 0.2 mmol/g and 0.1 mmol/g.

3.2 Membrane preparation

Membranes were prepared with a targeted thickness of 50 µm. Pure Nafion® membranes from the ION POWER dispersion, M112, and commercial N112 from Dupont, were considered as our reference to study the influence of the sepiolite incorporation in the composites. The pure Nafion® membrane labelled M112 was compared to the commercial

N112 membrane to evaluate the influence of our protocol of membrane preparation. Composite membranes were also prepared with pristine and sulfonated sepiolites (according to both protocols #1 and #2). Table 2 details the different membranes realized for this study.

Table 2: Membranes prepared for the study

Membrane label	Sepiolite	
	Type	Amount (wt%)
N112	-	0
M112	-	0
M112Sx	pristine	x = 05, 10, 20
M112SxS	Sepiolite#1	x = 05, 10, 20
M112SxSH	Sepiolite#2	x = 02, 05, 10

3.3 Membrane characterization

Our first concern was to evaluate the dispersion state of the sepiolite in the membrane. The micrograph of composite membrane prepared with pristine sepiolite does not show any visible sepiolite segregation within the thickness of the membrane (Figure 6.b).
Despite the use of a microtip to prepare the M112SxS series (sulfonation protocol #1), segregation has clearly been observed with the sulfonated sepiolite (Figure 6.c). On the contrary, the sulfonation protocol #2 developed for this study allowed avoiding such a segregation (M112SxSH series, Figure 6,d,).

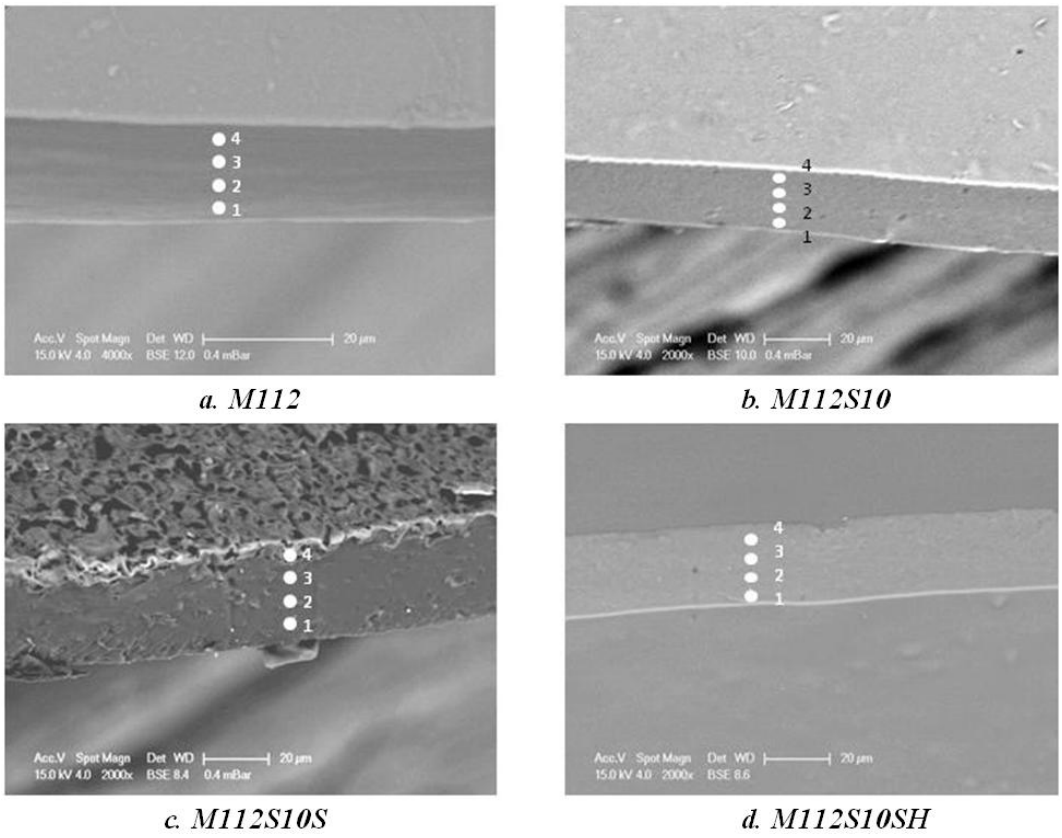


Figure 6: SEM micrographs of cryofractured membranes

These observations are confirmed with the qualitative chemical analysis (EDS) performed across the thickness of the membranes. Silicon, for sepiolite, and fluorine, for Nafion®, have been probed and the Si/F atomic ratio was calculated in order to check the sepiolite distribution within the membrane thickness (Table 3).

Table 3: Si/F atomic ratio (%) measured with EDS analysis at different position through the membrane.

Position	Si/F atomic ratio (%)		
	M112S10	**M112S10S**	**M112S10SH**
1	0.5	0.3	0.3
2	0.4	0.5	0.4
3	0.3	0.8	0.5
4	0.4	30	0.4

The Si/F atomic ratio is roughly constant across both M112S10 and M112S10SH membranes (points 1 to 4), thus confirming the good dispersion of fillers within the polymer matrix. On the contrary, the Si/F atomic ratio is highly inhomogeneous for M112S10S membrane, in agreement with SEM observation showing a strong segregation. The same phenomenon was observed with M112S20S (20 wt% of sepiolite).
The dispersion state of sepiolite has a direct influence on the mechanical resistance of the membrane. This has been checked by mechanical characterization.
It was assumed that the introduction of sepiolite could improve the mechanical resistance of the composite and thus its durability in FC operating conditions. The main results of the Dynamics Mechanical Analysis performed on our membranes are reported in Figure 7.

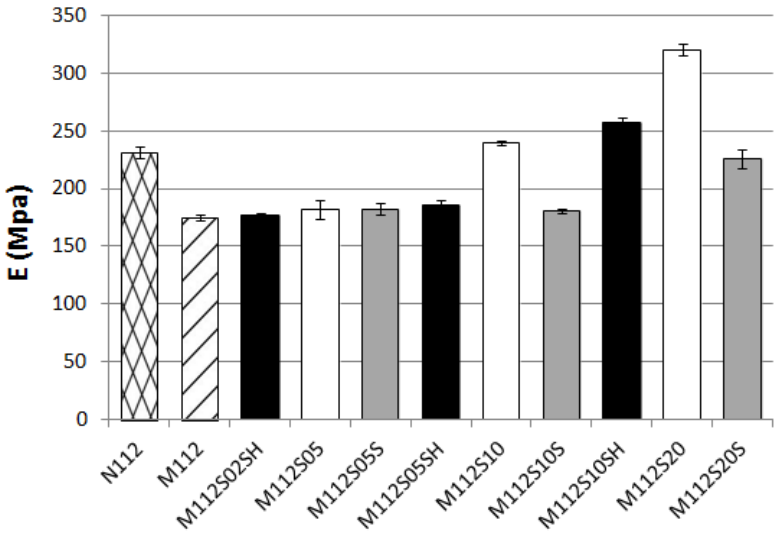


Figure 7. Elastic modulus measured for the different membranes by Dynamics Mechanical Analysis at 25 °C and 1 Hz.

The elastic modulus (E) is representative of the membrane tensile stiffness. M112 is significantly less stiff than N112, due to its elaboration process. In composites prepared with pristine sepiolite (M112Sx), the higher the sepiolite content the higher the stiffness. This confirms our assumption on the role of sepiolite in the composite, in good agreement with reported data on composite polymers [37]. This result is also consistent with the rather good dispersion of the sepiolite within the Nafion® matrix. On the contrary, the poor dispersion of the sulfonated sepiolite in the M112SxS series (sulfonation protocol #1) results in mechanical

properties which remain roughly similar to that of pure Nafion®. As already mentioned, the second sulfonation protocol (#2), developed for this study, allowed to homogeneously disperse the modified sepiolite within the Nafion® matrix. As a result, the elastic modulus of the M112SxSH series is increasing with the sepiolite content thus confirming the better dispersion of sepiolite observed in SEM.
As expected the reinforcing effect has been observed only with a satisfying dispersion of fillers within the matrix. When this condition is satisfied, the reinforcing occurs from 10 wt% of sepiolite in the composite.

The table 4 summarizes characterization results of the different membranes described in this study.

Table 4. Membrane characterization results (th = thickness, IEC = Ion Exchange Capacity, W_{ut} = water uptake and S = swelling)

Membrane	**th** +/-1 (µm)	**IEC**+/-10% (meq/g)	$\mathbf{W_{ut}}$ +/-0.5 (wt%)	**S** +/-0.5 (%)		
				s_1	s_2	*th.*
N112	56	0.9	25.3	6	5,3	8
M112	68	1.1	30	4	3	4,6
M112S02SH	48	1.2	32.2	3.8	3.7	4.2
M112S05	63	1.1	35	5,6	5,7	8,6
M112S05S	66	1.3	33,5	6,2	6,2	6,5
M112S05SH	44	1.2	34.3	4.8	4.9	6.8
M112S10	63	0.9	38,4	5,9	6,1	10,5
M112S10S	79	1.2	38,6	5,1	5,1	6,8
M112S10SH	48	1.2	38.4	6.5	6.3	10.4
M112S20	62	0.7	45,5	9	9	12,7
M112S20S	76	1.2	43,8	6,4	6,1	8,6

First of all, the thicknesses of the membranes are quite close to the target value, considering that the commercially available N112 is already 10% thicker than expected. During the membrane preparation, the amount of Nafion® dispersion has been adjusted for the M112SxSH series in order to reach the targeted 50 µm thickness.

It is noteworthy that all the features of our pure Nafion® membrane (M112), are slightly better than those of N112. In agreement with some reported data [45,46,47], the IEC and the water uptake are higher for M112 compared to N112, while the swelling is lower whatever the dimension of the membrane. This is probably due to differences in elaboration routes, the commercial N112 being prepared by extrusion.

The introduction of sepiolite in Nafion® reinforces mechanically our composites membranes. Another expected impact is the increase of the hygroscopic nature of the composites which will help the proton conduction. This should even be emphasized thanks to sepiolite functionalization.

As expected, the water uptake continuously increases with the sepiolite content in the composites. The same trend has been observed for the membranes swelling, which is, for all compositions, larger in the thickness dimension.
The increase of water uptake due to the introduction of sepiolite does not depend on the type of sepiolite. The water uptake is indeed very similar for all the composite membranes prepared with the same amount of sepiolite, regardless the type of sepiolite, modified or not. This means that the modification of sepiolite does not alter its ability to retain water in the composite. The gain in water uptake corresponds actually to roughly three times the amount of sepiolite (expressed in wt%) added in the membrane. For instance, an addition of 10 wt% of sepiolite leads to a 30 % increase of water uptake.

The IEC of composite membranes prepared with pristine sepiolite is decreasing with an increasing percentage of sepiolite. This effect is mainly due to a dilution effect, since the sepiolite is not proton conductive. The sulfonation of sepiolite, whatever the protocol, allowed increasing the IEC of composites membranes prepared with sepiolite#1 or #2. The IEC of the M112SxS series is notably higher than that of the M112SxSH one, probably because of the higher degree of sulfonation resulting from protocol#1.

Both the water uptake and the IEC increase, respectively due to the introduction of sepiolite and its sulfonation, are expected to improve the performances of MEAs prepared with composite membranes.

3.4 MEA single cell tests

The different membranes were used to realize MEAs which were then tested at 75 °C and 100 °C and between 25 % and 100 % RH. The different polarization curves are shown on Figures 8 to 12.

N112 was first tested to get some reference data. It is clear from Figure 8 that at 75 °C (solid lines) the performances decrease slightly with relative humidity whereas at 100 °C (dashed lines) the drop is much more significant. Indeed, at 75 % RH the performances are very similar at 75 °C and 100 °C. On the contrary, at 50 % RH a noticeable drop is observed at 100 °C compared to 75 °C. So, for N112, at low relative humidity, the performances are much lower at 100 °C than at 75 °C. This is consistent with different data reported for PFSA membranes in the literature, on the evolution, with temperature and relative humidity, of the proton conductivity [48,49] and also of the cell performances [50].

Concerning M112, in agreement with the results obtained on recast membranes e.g. by Adjemian et al. [15], the performances at 75°C are slightly better than those of N112 (Figures 9 and 13). Such a behavior is related to the already noticed better features of this membrane: higher IEC and better water uptake. A decrease of performances is here also observed with the decrease of the relative humidity, whatever the temperature. The aforementioned better features of M112 compared to those of N112 (IEC and water uptake), are however not strong enough levers to keep higher MEA performances at 100 °C. They are actually significantly lower. The preparation process (casting vs extrusion) may be responsible of the poorer performances of M112 observed at 100 °C.

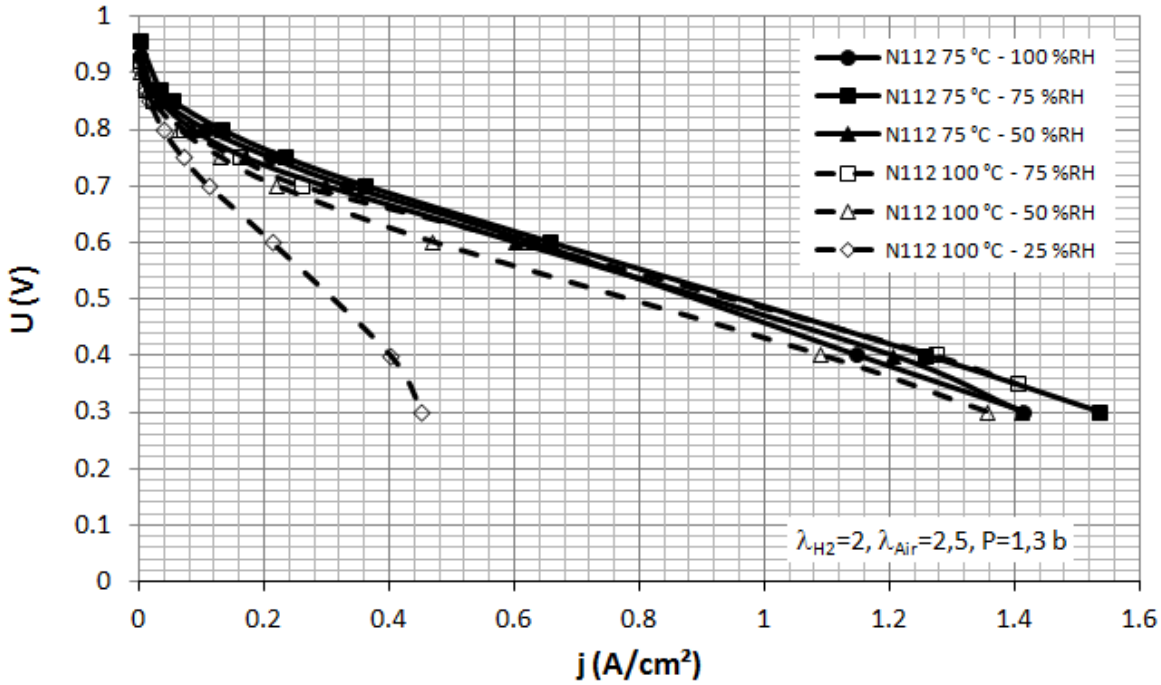


Figure 8. Polarization curves obtained for N112, at 75 °C (solid lines) and 100 °C (dashed lines), between 25 % and 100% relative humidity.

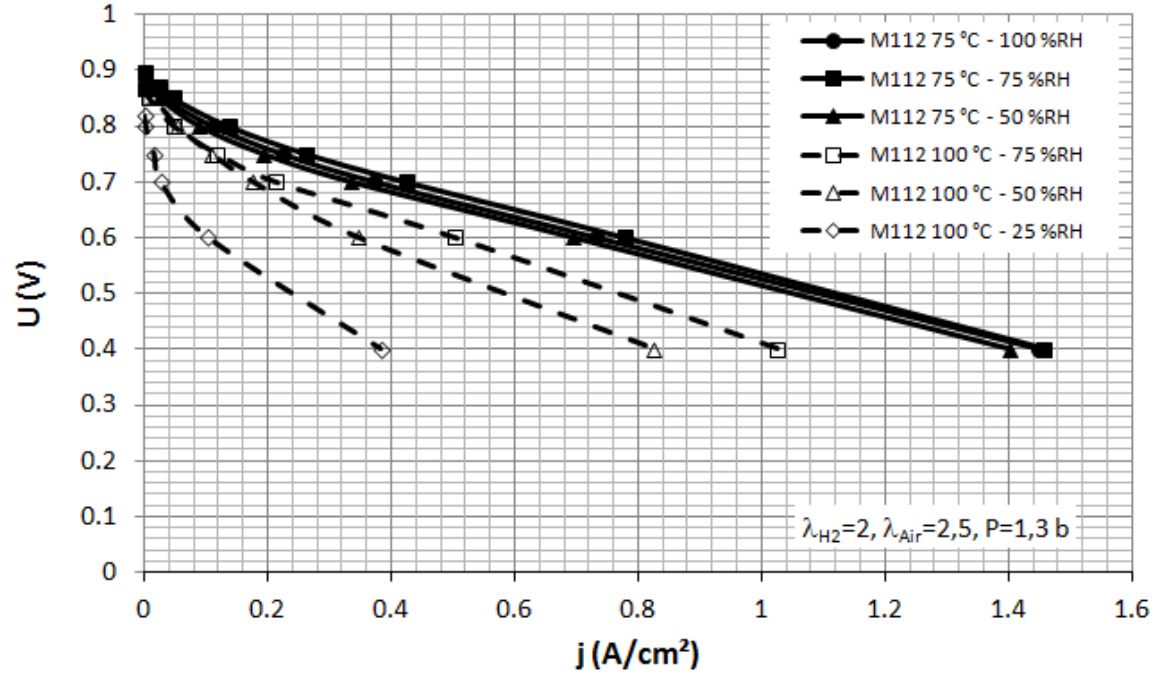


Figure 9. Polarization curves obtained for M112, at 75 °C (solid lines) and 100 °C (dashed lines), between 25 and 100% relative humidity.

This set of experiments leads to references useful to analyze the results obtained on composite membranes (Figures 10, 11 and 12).

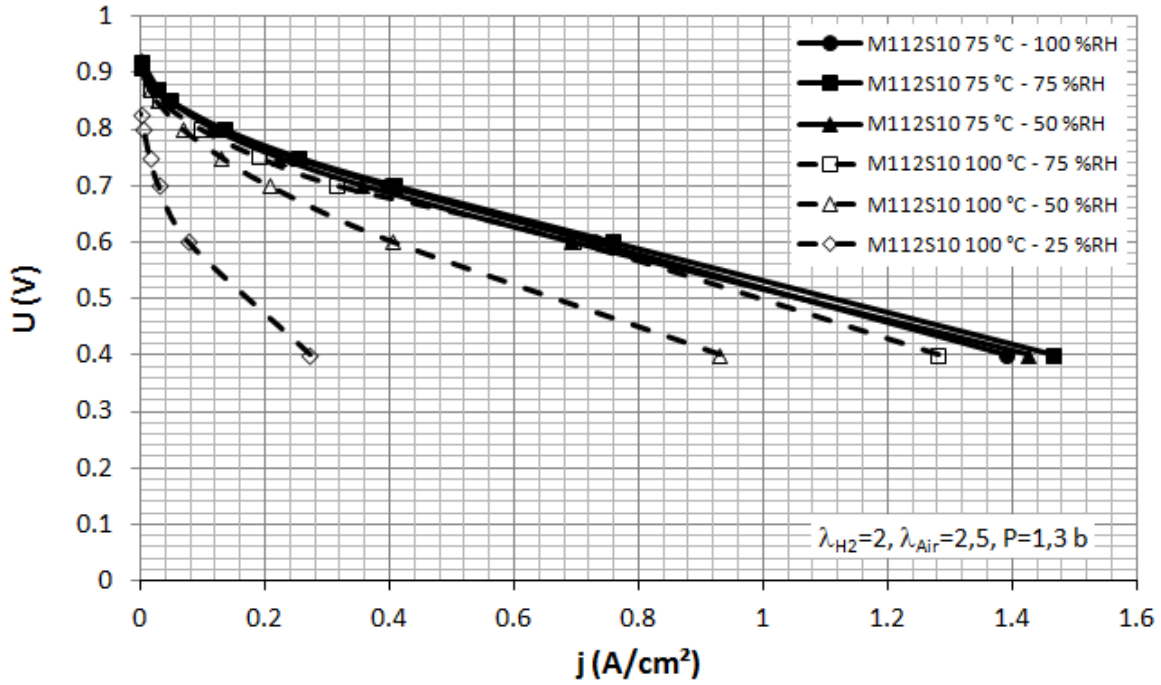


Figure 10. Polarization curves obtained for M112S10, at 75 °C (solid lines) and 100 °C (dashed lines), between 25 and 100% relative humidity.

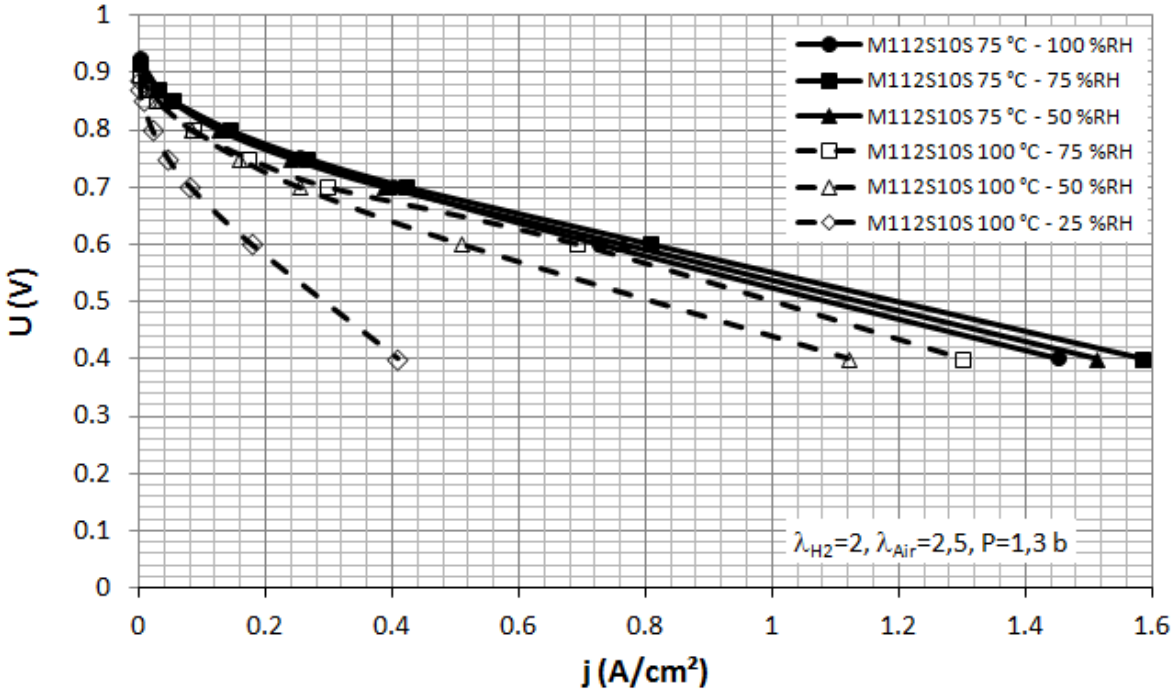


Figure 11. Polarization curves obtained for M112S10S, at 75 °C (solid lines) and 100 °C (dashed lines), between 25 and 100% relative humidity.

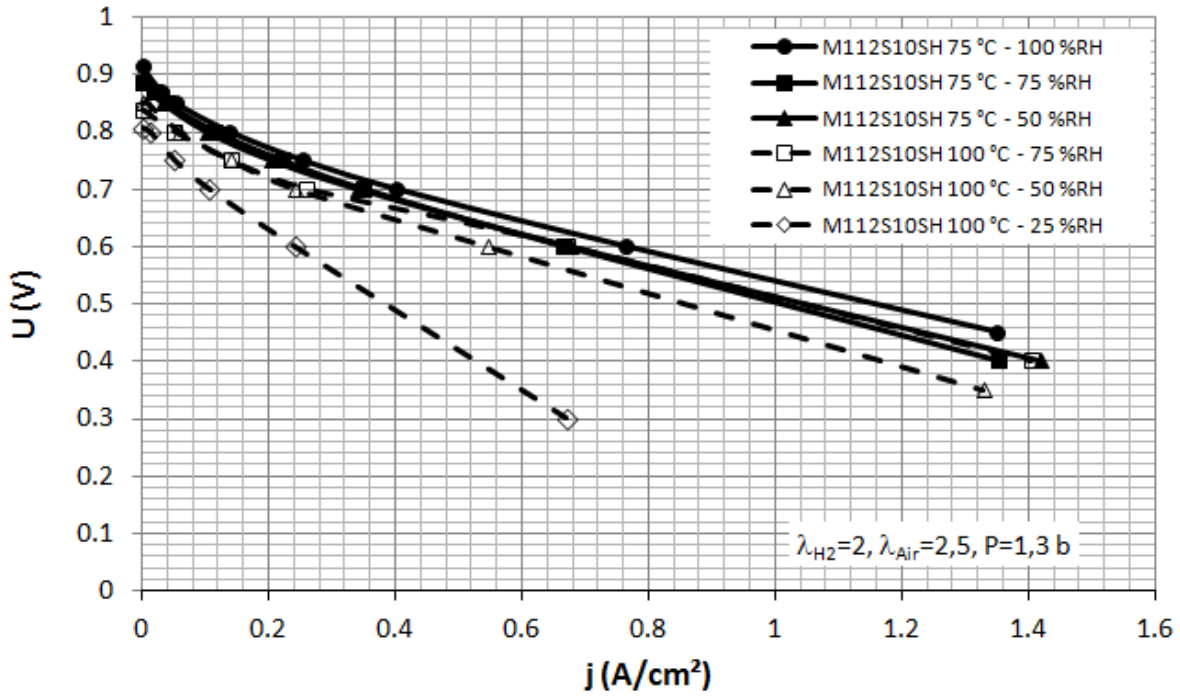


Figure 12. Polarization curves obtained for M112S10SH, at 75 °C (solid lines) and 100 °C (dashed lines), between 25 and 100% relative humidity.

From Figures 10 to 12, it can be noticed that the introduction of sepiolite in a Nafion® matrix has a significant impact on the performances of the corresponding MEA at 100 °C, whereas the impact at 75 °C is rather limited. The sulfonation of sepiolite was really beneficial since it allowed improving again the performances, especially at high temperature and low relative humidity.
Comparing Figure 9 (M112) and Figure 10 (M112S10), it is clear that the introduction of pristine sepiolite leads already to higher performances at 100 °C whereas the performances are similar at 75 °C. The sulfonation of sepiolite following the protocol #1 allowed improving the performances at 75 °C and 100 °C, especially at low relative humidity for the higher temperature. The sulfonation protocol developed for this study (#2) allowed reaching even much better performances at high temperature and low relative humidity. This improvement compared to M112S10S could also result from a thinner membrane. However, the improvement at 100 °C comparatively to 75 °C is more pronounced for M112S10SH than for M112S10S.

Provided that the different polarization curves do not cross each other, a convenient way to compare the results obtained here is to look at the current densities at a given voltage. Such a comparison was performed at 0.6 V and is illustrated on Figure 13.
Generally speaking, up to 75 % RH, the lower the relative humidity, the lower the current density at 0.6 V. This effect is more pronounced at high temperature.
At 75 °C, all recast membranes showed better performances than N112, even if, M112S10SH excepted, the membranes are thicker.
At 100 °C, as discussed previously, the unloaded recast membrane showed poorer performances than N112, but the introduction of sepiolite improves significantly its performances. Indeed, at 75 % RH, the current density at 0.6 V for M112S10 showed a 40 % increase compared to M112 and 12 % compared to N112. We assume this is due to the hygroscopic nature of sepiolite which retains water in the membrane, thus helping the proton conduction process.

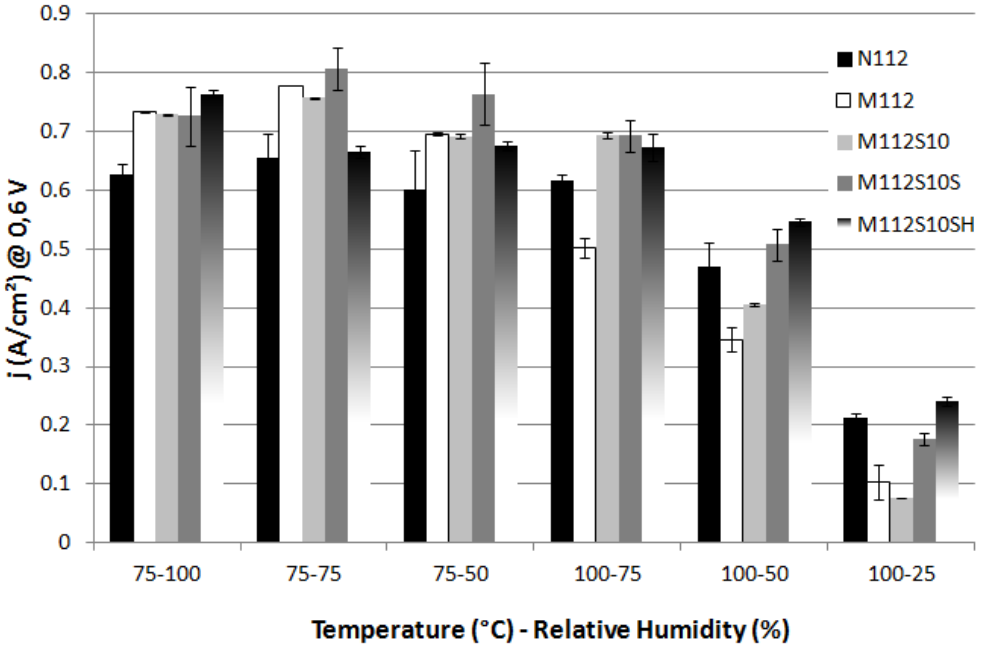


Figure 13. Influence of the temperature and the relative humidity (RH) on the current density at 0.6 V for the different membranes: N112 (black), M112 (white), M112S10 (light grey), M112S10S (dark grey) and M112S10SH (gradation), from left to right.

The sulfonation of sepiolite, whatever the protocol (#1 for M112S10S and #2 for M112S10SH), led to a further improvement of the performances (current density at 0.6 V), especially at high temperature and low relative humidity. Indeed, compared to M112, a 50% increase of the current density at 0.6 V was observed for M112S10S, at 100 °C and 50 % RH (60% for M112S10SH and 20% for M112S10 in the same conditions). At 100 °C and 25 % RH the increase is even larger: 70 % and 130 % respectively for M112S10S and M112S10SH, compared to M112. The water uptake of these composites is higher than that of M112, which could partially accounts for the better performance observed. Nevertheless the water uptake is similar for all 10 wt% composites and thus cannot be the unique responsible for the improvement observed. The different IEC (lower for M112S10 compared to M112 and higher for M112S10S and M112S10SH) may also partly explain the observed evolutions. Indeed, the sulfonation of sepiolite is supposed to favor the proton conduction through the membrane.
So both the hygroscopic nature of sepiolite and its sulfonation helped improving the membrane performances. These impacts are more pronounced at high temperature and low relative humidity.

A deeper analysis is necessary to discriminate the important membrane features which could impact the MEA performances. So the difference of performances discussed hereabove have been analysed based on complementary data obtained during the MEA single cell testing, namely the MEA resistance and the membrane hydrogen crossover. The MEA resistance (Figure 14.a) is directly linked to the membrane conductivity while the hydrogen crossover impacts the open circuit voltage (Figures 14.b and c). Thus low MEA resistance and low hydrogen crossover will lead to higher performances.

Among other operating conditions, the MEA resistance has been measured at open circuit voltage, under flowing H_2 at the anode and N_2 at the cathode.

As expected, whatever the temperature, the lower the relative humidity, the higher the resistance. No big difference was observed between 75 °C and 100 °C, keeping the same relative humidity.

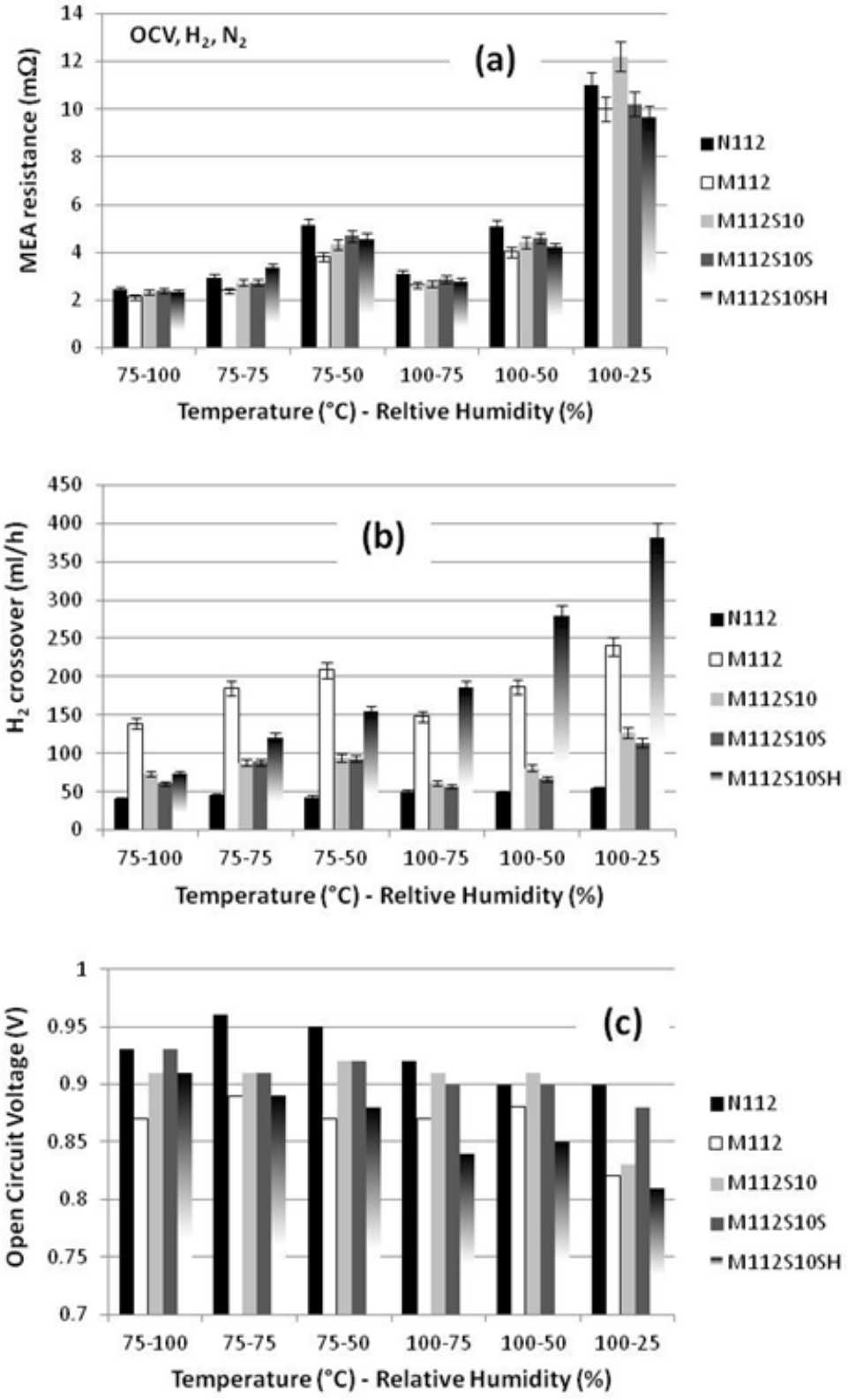


Figure 14. Influence of the temperature and the relative humidity (RH) on the MEA resistance (a), on the H_2 crossover (b) and on the open circuit voltage (c), for the different membranes [from the left to the right: N112 (black), M112 (white), M112S10 (light grey), M112S10S (dark grey) and M112S10SH (gradation)].

The introduction of sepiolite, pristine or sulfonated, in the membrane, entails only a very slight increase of resistance. As the performances of the corresponding MEA are generally improved with the introduction of sepiolite, it can be stated that such an increase of resistance is not limiting.
It is however interesting to notice that in severe conditions, namely 100 °C and 25 % RH, M112S10 exhibited a higher resistance, probably because the pristine sepiolite is not proton conductive. On the contrary the lower resistance of M112S10S and M112S10SH may be due to the proton conductivity of sepiolite induced by the sulfonation. The lower resistance of M112S10SH compared to that of M112S10S comes from the fact that the membrane is thinner. Since it was prepared with a less sulfonated sepiolite, we would indeed expect a higher resistance than M112S10S. These results are consistent with the evolution of the current density at 0.6 V previously discussed and confirm the beneficial effect of the sulfonation of sepiolite. Three parameters have to be considered here: the sulfonation degree of sepiolite, its distribution within the membrane and the thickness of the membrane. In M112S10S, the sepiolite#1 is less evenly distributed than sepiolite#2 in M112S10SH but its sulfonation degree is higher than that of sepiolite#2. With the same thickness, M112S10SH would have a higher resistance than M112S10S. So the sulfonation degree seems to be a major feature since, with comparable thickness, it would allow M112S10S to have a lower resistance than M112S10SH despite a poorer distribution of sepiolite within the membrane.

Another important parameter to be considered in performances analysis is the hydrogen crossover (Figure 14.b).
It is clear from Figures 14.b, and c that the higher the hydrogen crossover, the lower the open circuit voltage. The hydrogen crossover corresponds indeed to a loss of hydrogen for the electrochemical conversion. It is hence important to reduce the hydrogen crossover as much as possible.
It is noteworthy that for the majority of the composites, the sepiolite introduced in the Nafion® matrix entails a decrease of hydrogen crossover (increase of open circuit voltage) compared to that of M112, as already observed for different systems [51]. The resulting hydrogen crossover is even for some cases really close to that of N112. This is quite remarkable since recast membranes are known to be more permeable to hydrogen than commercial ones, accounting for the higher crossover observed for M112 compared to N112.
So the better performances of MEAs may also partly come from the decrease of hydrogen crossover entailed by the introduction of sepiolite.
The behavior observed for M112S10SH is different since a larger hydrogen crossover is observed. This is again partly due to the fact that the membrane is thinner. It could also result from a poorer interaction of sepiolite with Nafion. The function added on sepiolite following protocol #2 is indeed different both in size and chemical nature than that of protocol #1. We assume that this may be responsible for a weaker interaction with the polymer matrix, thus impacting the membrane "porosity" and so the hydrogen crossover. The interface between the polymer matrix and the fillers plays indeed a major role on hydrogen crossover [50]. Nevertheless, considering the FC tests results, especially at high temperature and low relative humidity, such a high crossover is not that detrimental and is compensated by a good distribution, contributing to a better conductivity, and a reduced thickness.

The membrane resistance and the hydrogen crossover should be both lowered by optimizing the thickness of the membrane, the sulfonation degree of sepiolite and by improving the compatibility between the filler, here sepiolite, and the polymer matrix, Nafion®.

4. Conclusion

Composite Nafion-sepiolite membranes realized in this study showed better performances than the pure Nafion membranes, especially at high temperature and low relative humidity.
Two protocols have been used in order to functionalize sepiolite and make it proton conductive. They gave rise to two different concentrations of sulfonic acid groups: 0.1 and 0.2 mmol/g.
The introduction of pristine sepiolite in Nafion® has shown some beneficial effects. On the one hand, the water uptake and the mechanical properties have been improved. On the other hand, the IEC has been decreased. Sulfonation of sepiolite to make it proton conductive has allowed limiting the decrease of IEC. Moreover, it led to improved fuel cell performances compared to composites prepared with pristine sepiolite. This is especially true at high temperature and low relative humidity, despite, in some cases, either a rather poor dispersion of the fillers in the Nafion® matrix (M112S10S) or a high resulting H_2 crossover (M112S10SH). The compatibility between sulfonated sepiolite and Nafion® should thus be optimized so as to increase the MEA performances (output power and durability through better mechanical resistance).
In the case of the M112Sx series, the expected increase of the hygroscopic nature of only one side of the membrane (the 30 % Si side), due to sepiolite segregation, may however be valorized to retain water at the anode side. This gradient of properties could both lower the electro-osmotic drag and increase the water diffusion from the cathode side where it is produced to the anode side.

Acknowledgements

The authors wish to thank the CARNOT MINES Institute and NANOMINES for financing this study and TOLSA SA for having provided sepiolite S9 and valuable technical data. They are also grateful to Patrick Leroux (CEP), Pierre Ilbizian (CEP), Michel-Yves PERRIN (CEMEF) and Suzanne JACOMET (CEMEF) for technical support.

References

[1] B. Bonnet, D.J. Jones, J. Roziere, L. Tchicaya, G. Alberti, M. Casciola, L. Massinelli, B. Bauer, A. Peraio, E. Ramunni, Hybrid organic-inorganic membranes for a medium temperature fuel cell, Journal of New Materials for Electrochemical Systems 3(2) (2000) 87-92.

[2] D.J. Jones, J. Roziere, Advances in the Development of Inorganic-Organic Membranes for Fuel Cell Applications, Fuel Cells I Advances in Polymer Science 215 (2008) 219-264.

[3] Q.F. Li, R.H. He, J.O. Jensen, N.J. Bjerrum, Approaches and recent development of polymer electrolyte membranes for fuel cells operating above 100 degrees C Chemistry of Materials 15(26) (2003) 4896-4915.

[4] J.M. Bae, I. Honma, M. Murata, T. Yamamoto, M. Rikukawa, N. Ogata, Properties of selected sulfonated polymers as proton-conducting electrolytes for polymer electrolyte fuel cells, Solid State Ionics 147 (2002) 189-194.

[5] R. Gosalawit, S. Chirachanchai, S. Shishatskiy, S.P. Nunes, Sulfonated montmorillonite/sulfonated poly(ether ether ketone) (SMMT/SPEEK) nanocomposite

membrane for direct methanol fuel cells (DMFCs) Journal of Membrane Science 323(2) (2008) 337-346.

[6] K.D. Kreuer, On the development of proton conducting polymer membranes for hydrogen and methanol fuel cells, Journal of Membrane Science 185(1) (2001) 29-39.

[7] J. Kerres, W. Cui, M. Junginger, Development and characterization of crosslinked ionomer membranes based upon sulfinated and sulfonated PSU - Crosslinked PSU blend membranes by alkylation of sulfinate groups with dihalogenoalkanes, Journal of Membrane Science 139(2) (1998) 227-241.

[8] F. Lufrano, I. Gatto, P. Staiti, V. Antonucci, E. Passalacqua, Sulfonated polysulfone ionomer membranes for fuel cells, Solid State Ionics 145(1-4) (2001) 47-51.

[9] P. Staiti, M. Minutoli, S. Hocevar, Membranes based on phosphotungstic acid and polybenzimidazole for fuel cell application, Journal of Power Sources 90(2) (2000) 231-235.

[10] C.H. Lee, S.Y. Hwang, J.Y. Sohn, H.B. Park, J.Y. Kim, Y.M. Lee, Water-stable crosslinked sulfonated polyimide-silica nanocomposite containing interpenetrating polymer network, Journal of Power Sources 163(1) (2006) 339-348.

[11] J. Peron, E. Ruiz, D.J. Jones, J. Rozières, Solution sulfonation of a novel polybenzimidazole. A proton electrolyte for fuel cell application, Journal of Membrane Science 314(1-2) (2008) 247-256.

[12] D.J. Jones, J. Roziere, Recent advances in the functionalisation of polybenzimidazole and polyetherketone for fuel cell applications, Journal of Membrane Science 185(1) (2001) 41-58.

[13] M. Watanabe, H. Uchida, Y. Seki, M. Emori, P. Stonehart, Self-humidifying polymer electrolyte membranes for fuel cells, Journal of the Electrochemical Society 143(12) (1996) 3847-3852.

[14] P.L. Antonucci, AS. Arico, P. Creti, E. Ramunni, V. Antonucci, Investigation of a direct methanol fuel cell based on a composite Nafion (R)-silica electrolyte for high temperature operation, Solid State Ionics 125(1-4) (1999) 431-437.

[15] K.T. Adjemian, S.J. Lee, S. Srinivasan, J. Benziger, A.B. Bocarsly, Silicon oxide Nafion composite membranes for proton-exchange membrane fuel cell operation at 80-140 degrees C, Journal of the Electrochemical Society 149(3) (2002) A256-A261.

[16] A.S. Aricò, P. Cretì, P.L. Antonucci, V. Antonucci, Comparison of ethanol and methanol oxidation in a liquid-feed solid polymer electrolyte fuel cell at high temperature, Electrochemical and Solid-State Letters 1 (2) (1998) 66-68.

[17] A. Sacca, A. Carbone, E. Passalacqua, A. D'Epifanio, E. Traversa, E. Sala, F. Traini, R. Ornelas, Nafion-TiO_2 hybrid membranes for medium temperature polymer electrolyte fuel cells (PEFCs), Journal of Power Souces 152(1) (2005) 16-21.

[18] N.H. Jalani, K. Dunn, R. Datta, Electrochimica Acta 51(3) (2005) 553-560.

[19] R.A. Zoppi, I.V.P. Yoshida, S.P. Nunes, Hybrids of perfluorosulfonic acid ionomer and silicon oxide by sol-gel reaction from solution: Morphology and thermal analysis, Polymer 39 (1998) 1309-1315.

[20] K.A. Mauritz, Organic-inorganic hybrid materials: perfluorinated ionomers as sol-gel polymerization templates for inorganic alkoxides, Materials Science and Engineering C-Biomimetic and supramolecular systems 6(2-3) (1998) 121-133.

[21] N. Miyake, J.S. Wainright, R.F. Savinell, Evaluation of a sol-gel derived Nafion/silica hybrid membrane for polymer electrolyte membrane fuel cell applications - II. Methanol uptake and methanol permeability, Journal of The Electrochemical Society 148(8) (2001) A905-A909.

[22] E. Peled, T. Duvdevani, A. Melman, A novel proton-conducting membrane, Electrochemical and Solid State Letters 1(5) (1998) 210-211.

[23] P. Staiti, A.S. Aricò, V. Baglio, F. Lufrano, E. Passalacqua and V. Antonucci, Hybrid Nafion-silica membranes doped with heteropolyacids for application in direct methanol fuel cells, Solid State Ionics 145 (2001) 101-107.

[24] Z.G. Shao, H. Xu, M.Q. Li, I.M. Hsing, Hybrid Nafion-inorganic oxides membrane doped with heteropolyacids for high temperature operation of proton exchange membrane fuel cell, Solid State Ionics 177 (2006) 779-785.

[25] M. Helen, B. Viswanathan, S.Srinivasa Murthy, Synthesis and characterization of composite membranes based on alpha-zirconium phosphate and silicotungstic acid, Journal of Membrane Science 292(1-2) (2007) 98-105.

[26] S. Shanmugam, B. Viswanathan, T.K. Varadarajan, Synthesis and characterization of silicotungstic acid based organic-inorganic nanocomposite membrane, Journal of Membrane Science 275(1-2) (2006) 105-109.

[27] G. Alberti, M. Casciola, R. Palombari, Inorgano-organic proton conducting membranes for fuel cells and sensors at medium temperatures, Journal of Membrane Science 172(1-2) (2000) 233-239.

[28] G. Alberti, M. Casciola, D. Capitani, A. Donnadio, R. Narducci, M. Pica, M. Sganappa, Novel Nafion-zirconium phosphate nanocomposite membranes with enhanced stability of proton conductivity at medium temperature and high relative humidity, Electrochemica Acta 52 (2007) 8125-8132.

[29] P. Costamagna, C. Yang, A.B. Bocarsly, S. Srinivasan, Nafion (R) 115/zirconium phosphate composite membranes for operation of PEMFCs above 100 degrees C, Electrochemica Acta 47(7) (2002) 1023-1033.

[30] F. Mura, R.F. Silva, A. Pozio, Study on the conductivity of recast Nafion (R)/montmorillonite and Nafion (R)/TiO_2 composite membranes, Electrochemica Acta 52(19) (2007) 5824-5828.

[31] Y.F. Lin, C.Y. Yen, C.H. Hung, Y.H. Hsiao, C.C.M. Ma, A novel composite membranes based on sulfonated montmorillonite modified Nafion® for DMFCs, Journal of Power Sources 168(1) (2007) 162-166.

[32] D.H. Jung, S.Y. Cho, D.H. Peck, D.R. Shin, J.S. Kim, Preparation and performance of a Nafion (R)/montmorillonite nanocomposite membrane for direct methanol fuel cell, Journal of Power Sources 18(1-2) (2003) 205-211.

[33] P. Bebin, M. Caravanier, H. Galiano, Nafion (R)/clay-SO_3H membrane for proton exchange membrane fuel cell application, Journal of Membrane Science 278(1-2) (2006) 35-42.

[34] F. Xu, S. Mu, M. Pan, Mineral nanofibre reinforced composite polymer electrolyte membranes with enhanced water retention capability in PEM fuel cells, Journal of Membrane Science 377 (2011) 134-140.

[35] G. Tartaglione, D. Tabuani, G. Camino, Thermal and morphological characterisation of organically modified sepiolite, Microporous and Mesoporous Materials 107 (2008) 161-168.

[36] F. Chivrac, E. Pollet, M. Schmutz, L. Avérous, Starch nano-biocomposites based on needle-like sepiolite clays, Carbohydrate Polymers 80(1) (2010) 145-153.

[37] F.J. Fernandez-Carretero, V. Compañ, E. Riande, Hybrid ion-exchange membranes for fuel cells and separation processes, Journal of Power Sources 173(1) (2007) 68-76.

[38] F.J. Fernandez-Carretero, E. Riande, C. del Rio, F. Sanchez, J.L. Acosta, V. Compañ, Preparation and Characterization of Hybrid Membranes based on Nafion (R) using Partially Sulfonated Inorganic Fillers, Journal of New Materials for Electrochemical Systems 13(2) (2010) 83-93.

[39] F.J. Fernandez-Carretero, K. Suarez, O. Solorza, E. Riande, V. Compañ, PEMFC Performance of MEAS Based on Nafion (R) AND sPSEBS Hybrid Membranes, Journal of New Materials for Electrochemical Systems 13(3) (2010) 191-199.

[40] G. Tartaglione, D. Tabuani, G. Camino, M. Moisio, PP and PBT composites filled with sepiolite: Morphology and thermal behaviour, Composites Science and Technology 68 (2008) 451-460.

[41] M. Ouattara-Brigaudet, C. Beauger, S. Berthon-Fabry, P.Achard, Carbon Aerogels as Catalyst Supports and First Insights on Their Durability in Proton Exchange Membrane Fuel Cells, Fuel Cells 11(6) (2011) 726-734

[42] W. Kuang, G.A. Facey, C. Detellier, B. Casal, J.M. Serratosa, E. Ruiz-Hitzky, Nanostructured hybrid materials formed by sequestration of pyridine molecules in the tunnels of sepiolite, Chemistry of Materials 15(26) (2003) 4956–4967.

[43] M. Alkan, G. Tekin, H. Namli, FTIR and zeta potential measurements of sepiolite treated with some organosilanes, Microporous and Mesoporous Materials 84(1-3) (2005) 75-83.

[44] C. Wan and B. Chen, Synthesis and characterization of biomimetic hydroxyapatite/sepiolite nanocomposites *Nanoscale* 3 (2011) 693-700.

[45] P. Dimitrova, K.A. Friedrich, U. Stimming, B. Vogt, Modified Nafion®-based membranes for use in direct methanol fuel cells, Solid State Ionics 150(1-2) (2002) 115-122.

[46] Z.G. Shao, P. Joghee, I.M. Hsing, Preparation and characterization of hybrid Nafion-silica membrane doped with phosphotungstic acid for high temperature operation of proton exchange membrane fuel cells, Journal of Membrane Science 229(1-2) (2004) 43-51.

[47] P. Dimitrova, K.A. Friedrich, B. Vogt, U. Stimming, Transport properties of ionomer composite membranes for direct methanol fuel cells, Journal of Electroanalytical Chemistry 532(1-2) (2002) 75-83.

[48] M. Doyle, S.K. Choi, G. Proulx, High-temperature proton conducting membranes based on perfluorinated ionomer membrane-ionic liquid composites, Journal of the Electrochemical Society , 147(1) (2000) 34-37.

[49] K.D. Kreuer, M. Schuster, B. Obliers, O. Diat, U. Traub, A. Fuchs, U. Klock, SJ. Paddison, J. Maier, Short-side-chain proton conducting perfluorosulfonic acid ionomers : Why they perform better in PEM fuel cells, Journal of Power Sources 178(2) (2008) 499-509.

[50] H. Tang, Z. Wan, M. Pan, S.P. Jiang, Self-assembled Nafion-silica nanoparticles for elevated-high temperature polymer electrolyte membrane fuel cells, Electrochemistry Communications 9(8) (2007) 2003-2008.

[51] K.T. Adjemian, S. Srinivasan, J. Benziger, A.B. Bocarsly, Investigation of PEMFC operation above 100˚C employing perfluorosulfonic acid silicon oxide composite membranes. Journal of Power Sources 109 (2002) 356-364.